Patchy environment as a factor of complex plankton dynamics

Alexander B. Medvinsky,* Irene A. Tikhonova, and Rubin R. Aliev
Institute for Theoretical & Experimental Biophysics, Pushchino, Moscow Region, 142290 Russia

Bai-Lian Li
Department of Biology, University of New Mexico, Albuquerque, New Mexico 87131-1091

Zhen-Shan Lin
Department of Geography, Nanjing Normal University, Nanjing 210093, People's Republic of China

Horst Malchow
Institut für Umweltsystemforschung, Artilleriestraße 34, 49069 Osnabrück, Germany
(Received 1 March 2001; published 26 July 2001)

We study the role of the diffusive interaction in plankton dynamics in a patchy environment. We use a minimal reaction-diffusion model of the nutrient—plankton—fish food chain to simulate the diffusive interaction between fish-populated and fish-free habitats. We show that such interaction can give rise to spatiotemporal plankton patterns. The plankton dynamics depend on the fish predation rate and can exhibit both regular and chaotic behavior. We show that limit cycle and chaotic attractor coexist in the system. The entire basin of attraction of the limit cycles is found to be riddled with ''holes'' leading to the competitive chaotic attractors. The chaotic dynamics is typical of a wide range of the fish predation rates.

DOI: 10.1103/PhysRevE.64.021915 PACS number(s): 87.23.Cc, 05.45.Pq, 92.20.Rb

I. INTRODUCTION

There is a growing interest in the chaotic dynamics of ecological systems [1]. In this paper we focus on the chaotic and regular dynamics of plankton populations in a patchy environment. Most of the works concerned with the temporal behavior of a biological community do not take into account its spatial structure. However, the spatial distribution of natural populations is usually remarkably inhomogeneous. In terrestrial ecosystems, the inhomogeneity of the spatial distribution of the populations is to a large extent controlled by the inhomogeneity of the environment. Very high mobility of the marine environment would prevent the formation of any stable patchy spatial distribution with much longer life-time than the typical times of the biodynamics. However, in addition to very changeable transient spatial patterns, in marine environment there also exist other, much more stable structures associated with ocean fronts [2,3], cyclonic rings [4], and so-called meddies [5]. This fact creats the biological basis for considering the dynamics of marine communities in a patchy environment. In this connection, it should be noted that the temporal dynamics of a community can depend significantly on the spatial structure of its environment [6–8].

Conceptual minimal models are an appropriate tool for searching and understanding basic mechanisms of spatial pattern formation and temporal dynamic behavior of interacting chemical substances or biological species. Such an approach goes back to the classic paper by Turing [9], where it has been shown that the nonlinear interaction of at least two agents with considerably different diffusion coefficients can give rise to spatial structure. Segel and Jackson [10] were the first to apply Turing's idea to ecology, having considered the dissipative instability in the predator-prey interaction of phytoplankton and herbivorous copepods with higher herbivore motility. Levin and Segel [11] suggested this scenario of spatial pattern formation as a possible origin of planktonic patchiness. The usefulness of minimal models has been demonstrated in the following studies of plankton patchiness and phytoplankton blooms [12,13,15,17]. Recently, the effects of external hydrodynamical forcing in the appearance of nonequilibrium spatiotemporal plankton patterns were studied [19–21]. Conceptual models have been also applied to investigate the plankton pattern formation resulting from planktivorous fish school walks without any hydrodynamical forcing [7,22,23] and the formation of irregular self-sustained spatial patterns uncorrelated with the properties of the environment [24,25]. Predator-prey limit-cycle oscillations, plankton fronts propagation, and the generation and drift of planktonic Turing patches were found in a minimal phytoplankton-zooplankton interaction model [26,27] that was originally formulated by Scheffer [28]. The emergence of diffusion-induced chaos has been found by Pascual [29] along a linear nutrient gradient in the same model without fish predation.

In this paper, using a one-dimensional (1D) minimal reaction-diffusion model of the nutrient – phytoplankton – zooplankton – fish food chain we show that:

(1) The diffusive interaction between different habitats in a patchy marine environment, while some of the patches are populated by fish and others may be fish free, can give rise to plankton spatial patterns;

(2) Plankton dynamics depend on the fish predation rate and can exhibit regular and chaotic behavior. Coexistence of a limit cycle and a chaotic attractor with Cantor setlike ba-

*Email address: medvinsky@venus.iteb.serpuknov.su

sins of attraction is characteristic of the model chaotic plankton dynamics. The chaotic dynamics is typical for a wide range of parameters.

II. MODEL

We consider the 1D two-component basic marine food chain model where at any point X and time τ, the dynamics of phytoplankton $P(X,\tau)$ and zooplankton $H(X,\tau)$ populations are given by the following reaction-diffusion equations [26,28–30]:

$$\frac{\partial P}{\partial \tau} = RP\left(1-\frac{P}{K}\right) - \frac{AC_1P}{C_2+P}H + D_P\Delta P, \tag{1}$$

$$\frac{\partial H}{\partial \tau} = \frac{C_1P}{C_2+P}H - MH - F\frac{H^2}{C_3^2+H^2} + D_H\Delta H. \tag{2}$$

Here, F is the fish predation rate on zooplankton. The parameters R, K, M, and $1/A$ denote the intrinsic growth rate, carrying capacity of phytoplankton, the death rate, and yield coefficient of phytoplankton to zooplankton, respectively. The constants C_1, C_2, and C_3 parametrize the saturating functional response. D_P and D_H are the diffusion coefficients of phytoplankton and zooplankton, respectively. Δ is the Laplace operator. The dependence of the zooplankton grazing rate on phytoplankton is of type II, while the zooplankton predation by fish follows a sigmoidal functional response of type III (according to [28,31]). The model can be simplified by introducing dimensionless variables. Following Pascual [29], we introduce $p=P/K$ and $h=AH/K$. Space is scaled by the size of the numerical mesh L/k, where L is the total length of the considered area and $k+1$ is the number of nodes of the mesh. Thus, L/k is the scale of the expected patterns. Time is scaled by a characteristic value of the phytoplankton growth rate R_0. Thus, $x=kX/L$, and $t=R_0\tau$. As a result, Eqs. (1) and (2) become

$$\frac{\partial p}{\partial t} = rp(1-p) - \frac{ap}{1+bp}h + d_p\Delta p, \tag{3}$$

$$\frac{\partial h}{\partial t} = \frac{ap}{1+bp}h - mh - f\frac{nh^2}{n^2+h^2} + d_h\Delta h, \tag{4}$$

where the new parameters are $r=R/R_0$, $a=C_1K/(C_2R_0)$, $b=K/C_2$, $m=M/R_0$, $n=C_3A/K$, $d_p=k^2D_P/(L_2R_0)$, $d_h=k^2D_H/(L_2R_0)$, $f=FA/(C_3R_0)$.

Considering the dynamics of the plankton community in a spatially structured marine environment suggests that the parameters in Eqs. (3) and (4) are coordinate dependent. In this paper we assume that the inhomogeneity of the environment affect only the fish population, i.e., the fish predation rate $f=f(x)$, whereas all other parameters are constant. For the sake of simplicity, we assume that f is equal to a certain constant value in the fish-populated patches, otherwise $f=0$.

The diffusion terms in Eqs. (1) and (2) often describe the spatial mixing of the species due to the self-motion of the organisms [32]. However, in natural waters it is turbulent diffusion that is supposed to dominate plankton mixing [30]. Taking this into account, we consider both phytoplankton and zooplankton as passive contaminants of the water turbulent motion. In this case $d_p=d_h=d$. Using the relationship between turbulent diffusivity and the scale of the phenomenon in the sea [30], with the minimum phytoplankton growth rate R_0 given by 10^{-6} sec^{-1} (cf. [33]), the characteristic length L/k of about $2km$ typical of plankton patterns, one can show that d is about 5×10^{-2}.

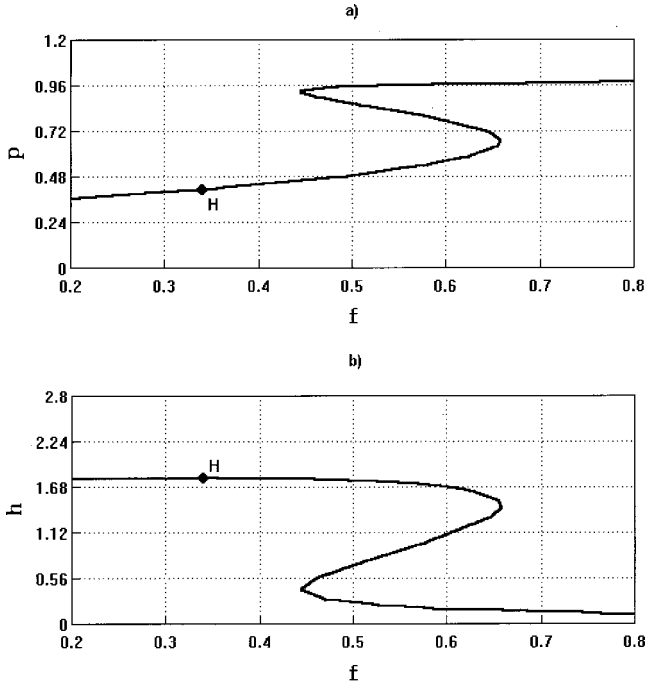

FIG. 1. Solution diagrams of the models (3) and (4) for the following set of parameters: $r=5$, $a=5$, $b=5$, $m=0.6$, $n=0.4$. This set of parameters is used throughout the work. The curves display the steady-state solutions for different values of f. H denotes a Hopf bifurcation.

For numerical integration of Eqs. (3) and (4), a simple explicit difference scheme is used. The 1D space is divided into a grid of 64 finite-difference cells of unit length. The border between habitats divides the space into two patches. The time step is set equal to 10^{-2}. Repetition of the integration with smaller step size showed that the numerical results did not change, ensuring the accuracy of the chosen time step. The plankton dynamics is investigated with no-flux boundary conditions. The initial distributions for h and p are uniform and the same for both the habitats.

III. THE DEPENDENCE OF THE SPATIOTEMPORAL PLANKTON DYNAMICS ON THE FISH PREDATION RATE

Figure 1 demonstrates the solution diagrams of the systems (3) and (4), i.e., the dependence of the steady-state solution (under $d_p=d_h=0$) on the fish predation rate. One can see that the phytoplankton-dominated stationary states are typical for high fish predation rate f. When lowering f, an unstable and another stable steady-state appear, which makes

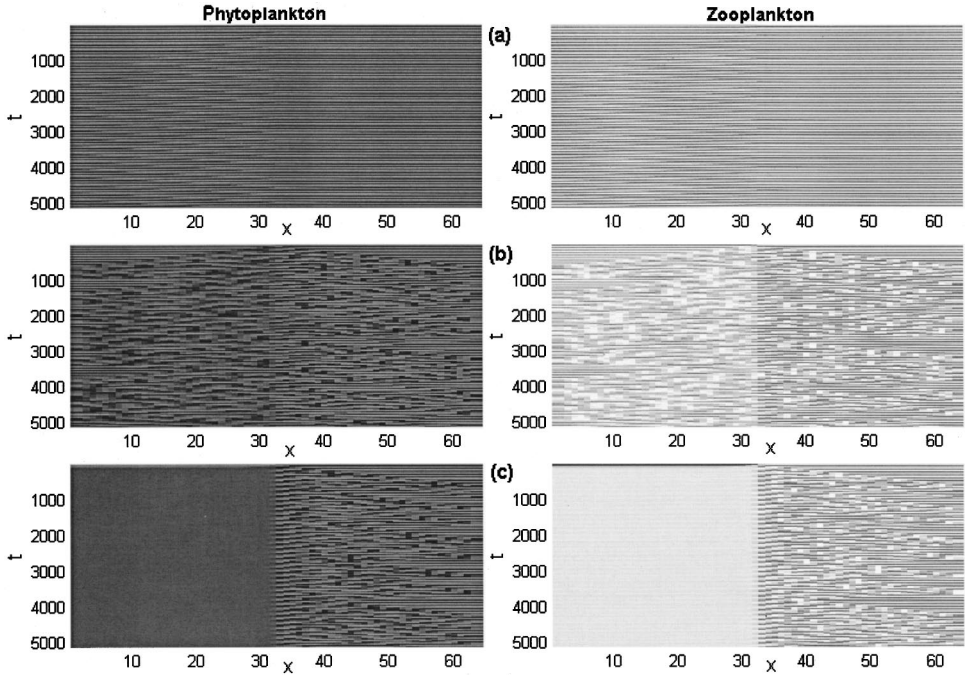

FIG. 2. Spatiotemporal plankton patterns emerged from initially homogeneous plankton distributions in the two-habitat system for (a) $f=0.05$, (b) $f=0.18$, and (c) $f=0.395$; x is the spatial coordinate, t is time. The darker regions correspond to lower plankton densities.

the system bistable. Further lowering f, the bistability disappears in a saddle-node bifurcation. For a lower value of f, at point H, a Hopf bifurcation occurs, destabilizing the zooplankton-dominated steady-state while creating a stable limit cycle. Particularly, it means that in the absence of fish ($f=0$), the local kinetics of the system is oscillatory (for all other parameters, as in Fig. 1). Notice that at $d_p=d_h$, both a stable steady state and a stable limit cycle of a ''point'' system are kept for a homogeneous distribution.

The sophisticated treatment of local properties of models similar to the models (3) and (4) have been carried out in works [20,28,34,35].

Let us consider the simplest example of a spatially structured ecosystem consisting of two patches only. The dynamics in both the patches obeys Eqs. (3) and (4), and in one of the patches $f=0$, i.e., fish is absent (for example, due to local changes in temperature or salinity). Figure 2 shows three sets of the 1D plankton spatial patterns that have been emerged from initially (at $t=0$) homogeneous plankton distributions as a result of the diffusion interaction of the habitat populated by fish (for $x\leqslant 32$) with $f=0.05$ [Fig. 2(a)], $f=0.18$ [Fig. 2(b)], and $f=0.395$ [Fig. 2(c)], and the patch ($x>32$) where fish is absent ($f=0$). It is readily seen (cf. Fig. 1) that the values $f=0.05$ and $f=0.18$ correspond to oscillatory plankton kinetics, while $f=0.395$ corresponds to the zooplankton-dominated steady state. One can see that increase of the fish predation rate is followed by transitions from rather regular plankton patterns [see Fig. 2(a) for $f=0.05$] to irregular ones [Fig. 2(b) for $f=0.18$] and then to virtually unstructured plankton distributions [Fig. 2(c) for $f=0.395$] in the fish-populated habitat, and from regular [Fig. 2(a)] to irregular [Figs. 2(b),2(c)] patterns in the fish-free habitat. Note that the interaction between the patches is essential to disturb the initially homogeneous distributions, otherwise no pattern could occur. Hence, pattern formation may be due to diffusive interactions of the spatially distributed systems with different local dynamics.

In order to demonstrate the dependence of the plankton spatial patterns on the fish predation rate in more detail, we construct the pattern bifurcation diagram. Figure 3 shows the plankton abundance as a function of position x (the horizontal axis) calculated at $t=5000$ for different values of f (the vertical axis) from $f=0$ to $f=0.395$. One can see that for the fish-populated habitat, the structures with larger inner scale characteristics for the smaller f transform into small-scale irregular patterns as f is growing, and then to the nearly homogeneous plankton distributions as the local dynamics of the system passes through the Hopf bifurcation, cf. Fig. 1. In contrast, in the fish-free habitat the Hopf bifurcation is not accompanied by essential changes in plankton spatial structure (Fig. 3).

IV. TEMPORAL DYNAMICS OF THE PLANKTON ABUNDANCE

To study temporal dynamics of the plankton abundance, we use values $|\mathbf{p}_i(t)|$ and $|\mathbf{h}_i(t)|$, i.e., the length of the vectors characterizing phytoplankton and zooplankton density distributions in each of the habitats:

$$\mathbf{p}_i(t)=[p_{i1}(t),p_{i2}(t),\ldots,p_{ik/2}(t)], \tag{5}$$

$$\mathbf{h}_i(t)=[h_{i1}(t),h_{i2}(t),\ldots,h_{ik/2}(t)], \tag{6}$$

where $i=1$ corresponds to the fish-populated habitat, $i=2$ to the fish-free one, k is the number of cells of the numerical mesh.

It emerges that the temporal dynamics of $|\mathbf{p}_i|$ and $|\mathbf{h}_i|$ depends significantly on the fish predation rate f. As an example, Figs. 4(a) and 4(b) demonstrate the temporal dynamics of zooplankton densities for fish-populated and fish-free patches, correspondingly. There exist three main types of the

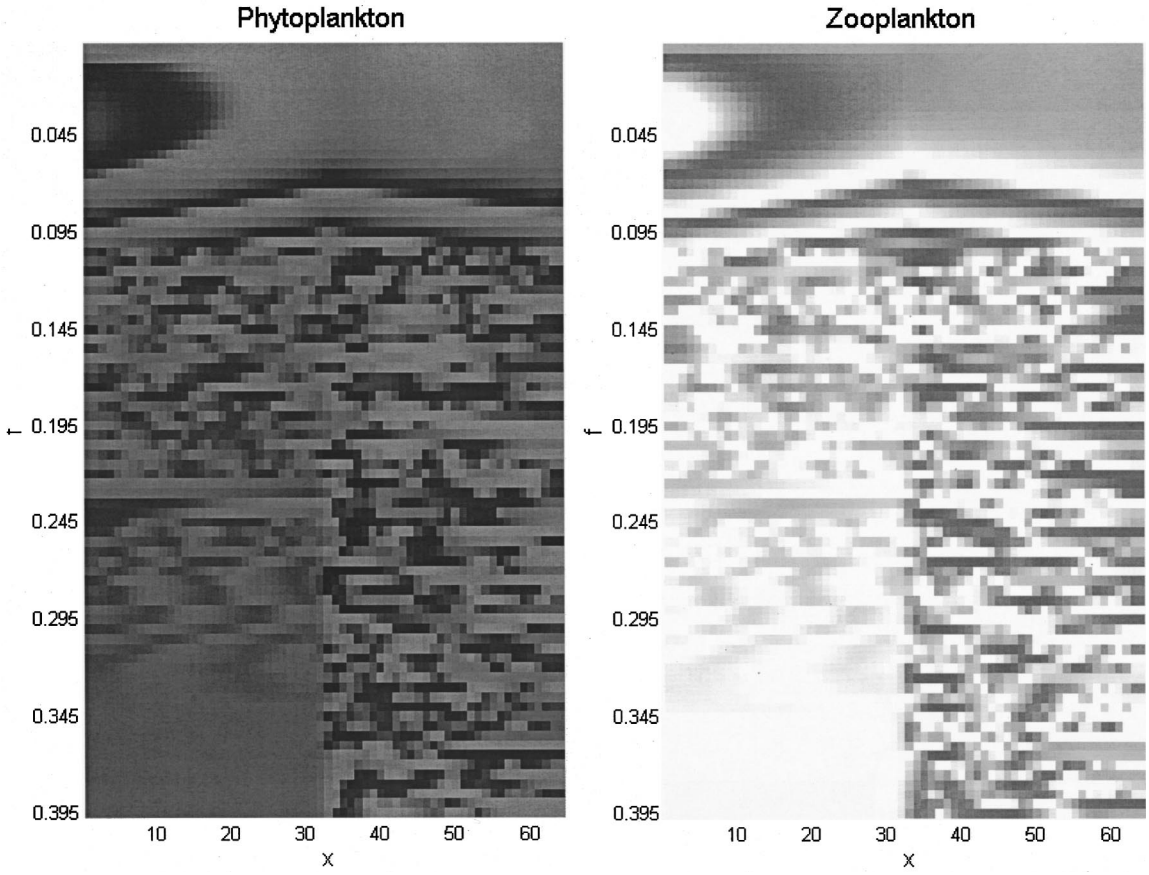

FIG. 3. Pattern bifurcation diagrams for phytoplankton and zooplankton obtained after 500 000 iterations; x is the spatial coordinate, f is the fish predation rate. These diagrams are shown in the same gray color scale as patterns in Fig. 2.

dynamics: (i) regular oscillations (when f is small); (ii) irregular oscillations in both fish-populated and fish-free patches (as f increases); (iii) virtually constant plankton density in the fish-populated patch while irregular oscillations appear in the fish-free habitat (when f undergoes further growth and becomes larger than the critical value characteristic of the Hopf bifurcation; see Fig. 1). The temporal behavior of the phytoplankton density $|\mathbf{p}_i|$ is qualitatively the same. Notice the increase of the averaged in time level of zooplankton as f is growing (Fig. 4). It is likely due to diffusion of phytoplankton that zooplankton is grazing on from the fish-free habitat where phytoplankton abundance is higher (not shown) into the fish-populated one where phytoplankton abundance is lower.

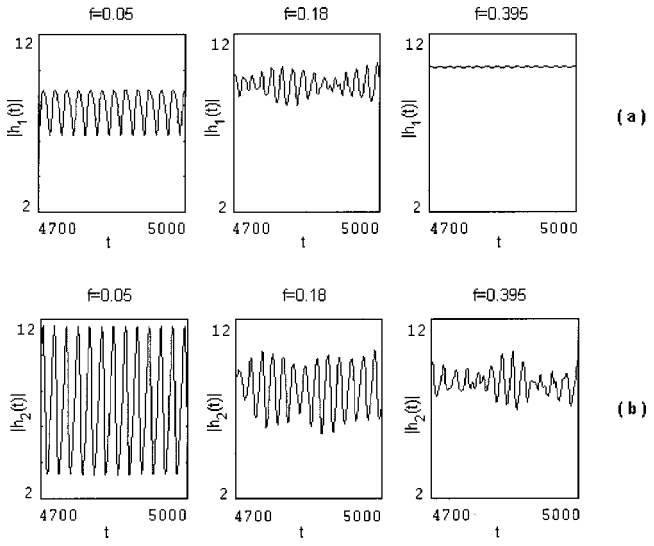

FIG. 4. Three main types of oscillations of the values $|\mathbf{h}_1(t)|$ and $|\mathbf{h}_2(t)|$ depending on f. (a) At $x \leqslant 32$ (fish-populated habitat) and (b) at $x > 32$ (fish-free patch).

One can see a clear correspondence between the three types of the temporal behavior of the densities $|\mathbf{h}_i|$ (Fig. 4) and the spatiotemporal patterns in Fig. 2. Namely, regular and irregular patterns lead to regular and irregular oscillations of $|\mathbf{p}_i|$ and $|\mathbf{h}_i|$, respectively, while nearly homogeneous patterns lead to virtually constant plankton density. It should be mentioned that not only a type of temporal behavior but also the range of regular oscillations of $|\mathbf{p}_i|$ and $|\mathbf{h}_i|$ depends on the fish predation rate (Fig. 5).

It is noteworthy that in contrast to regular regimes irregular ones are characterized by positive values of at least four first Lyapunov exponents (see Appendix, Tables I and II). This implies high-dimensional chaos responsible for the irregular plankton dynamics.

In order to demonstrate the chaotic nature of the plankton dynamics in more detail we study the dependence of the

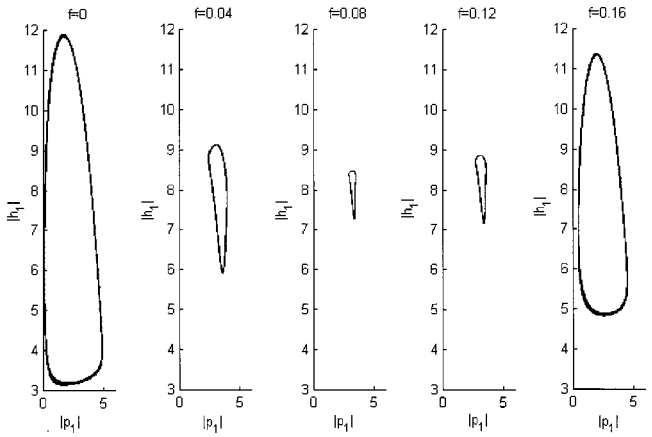

FIG. 5. The dependence of regular oscillations of $|\mathbf{p}_1(t)|$ and $|\mathbf{h}_1(t)|$ on the fish predation rates.

plankton oscillations on initial conditions. Figure 6 shows two attractors obtained at slightly different initial zooplankton densities but under the same set of the model parameters. One can see that very small changes in starting conditions can lead to both regular oscillations of the plankton abundance [Fig. 6(a)] and the chaotic plankton dynamics. Thus, there are two basins of attraction, one associated with each of the two attractors.

Interestingly, there is a large region of the initial zooplankton densities for which the basin of attraction to the limit cycle is interleaved in a complicated way with the basin of chaotic attractor. To demonstrate this, we consider the plankton dynamics starting from a sequence of initial zooplankton densities. Figure 7 shows which initial conditions lying in the range between 0.3 and 2.7 lead to the limit cycle [Fig. 6(a)] and which ones to the chaotic attractor [Fig. 6(b)]; initial conditions that approach the chaotic attractor are shaded white while all the initial densities leading to regular oscillations are shaded black. One can see that zooming in on a section of the whole range (for example, $1.8 \leqslant |\mathbf{h}_1(0)| = |\mathbf{h}_2(0)| \leqslant 2.55$) reveals additional structure and shows that the seemingly continuous black zones are in fact broken into smaller ones. As we try to define more precisely the boundary between the basins of attraction, we see an increasingly fractured boundary (Fig. 7). The basins of attraction from these zooplankton densities for both regular and chaotic oscillations are fractal—and are a type of Cantor set. But there is a region of initial zooplankton densities adjacent to $h_1(0)=h_2(0)=2.7$ that is continous, nonfractal. All the trajectories starting from this region lead to the chaotic attractor (Fig. 7).

V. CONCLUDING REMARKS

Recently, we have shown that plankton patchiness can be influenced by spatiotemporal fish dynamics [7,22,23]. In turn, fish-school behavior is found to be dependent on the plankton spatiotemporal dynamics [7,14,16,18,23,37]. The results presented in this paper show that plankton patchiness can be due to fish abundance gradients in the patchy environment. Hence, fish-plankton interplay, along with hydrodynamic factors [19–21] can be considered as an essential element of spatiotemporal plankton community functioning.

Plankton communities often show large fluctuations in both zooplankton and algal biomass. Such irregular patterns can be sometimes explained by inaccurate sampling or by stochastic environmental effects on the population under study. At the same time, irregularity in plankton dynamics can be due to the chaotic rather than stochastic nature of the processes underlying spatiotemporal changes in the plankton abundance. Unfortunately, it is not easy to find experimental support for chaos in aquatic communities. However, the analysis of field data [36] indicates that the recorded dynamics of diatom communities can be chaotic. Our results show that irregular plankton dynamics can arise as a result of the coexistence of at least two attractors with Cantor setlike basins of attraction. It is difficult if not impossible to predict which basin will attract a particular trajectory unless very precise information is available about the initial conditions (see Fig. 7). Even weak external noise renders the system unpredictable. Our results also show that chaotic plankton

TABLE I. Values of λ_1. a,b,c,d correspond to the zooplankton distributions shown in Fig. 8.

a	b	c	d
0.0172	0.0166	0.0171	0.0165

TABLE II. Values of λ_2. a,b,c,d correspond to the zooplankton distributions shown in Fig. 8.

Zooplankton distributions	a	b	c
b	0.0163		
c	0.0169	0.0172	
d	0.0164	0.0160	0.0165

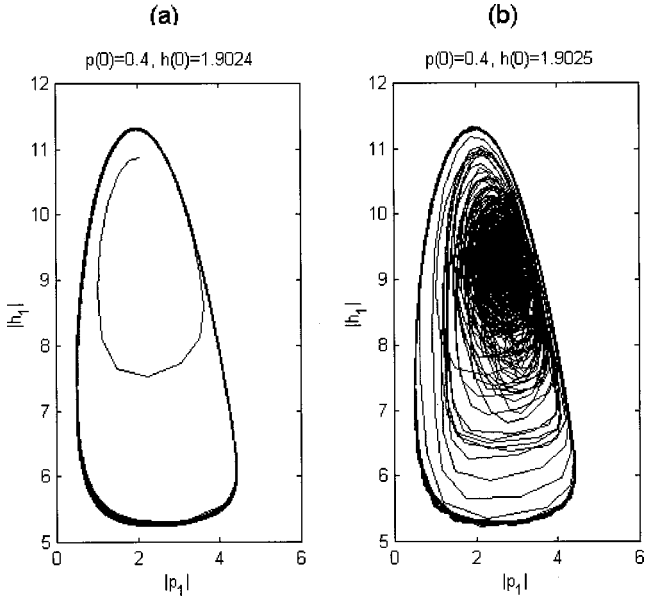

FIG. 6. Sensitivity to initial conditions. The stable limit cycle (a) and chaotic attractor (b) are obtained at slightly different initial zooplankton densities differing only by 0.0001. Here $f=0.18$.

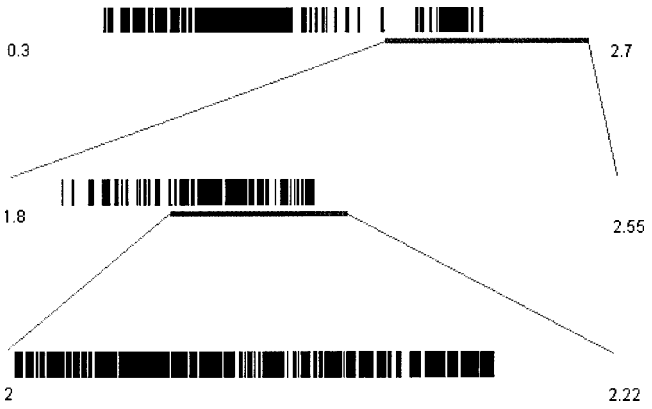

FIG. 7. Fractal structure of the attractor basins. Initial conditions that approach the chaotic attractor are shaded white, and initial conditions leading to regular oscillations are shaded black.

dynamics and corresponding irregular spatial patterns can be found in a wide region of the values of the fish predation rate (Figs. 2–4). This may indicate the vital role of chaotic regimes in the spatiotemporal organization of aquatic ecosystems.

ACKNOWLEDGMENTS

The authors acknowledge helpful discussions with Dr. S. V. Petrovskii (Moscow), Professor E. E. Shnol (Pushchino), and Professor E. Venturino (Torino). This research was supported by DFG, NSF, and RFBR grants.

APPENDIX

The maximal Lyapunov exponent λ_1 is well known to be determined in the following way. Let $h(t)$ and $h^0(t)$ be two points in state space with distance $\delta(t)=\|h(t)-h^0(t)\|$, $\delta(t_1)\ll 1$; $t\in[t_1,t_2]$ (here $t_1=450.01$; $t_2=1250$) between the two trajectories going through these points at time t. To specify the distance $\delta(t)$, we use four different vectors $\mathbf{h}^{(1)}(t)$, $\mathbf{h}^{(2)}(t)$, $\mathbf{h}^{(3)}(t)$, and $\mathbf{h}^{(4)}(t)$ describing zooplankton distributions slightly disturbed at the moment t_1 as it is shown in Fig. 8, and the vector $\mathbf{h}^{(0)}(t)$ describing undisturbed zooplankton distribution as a "control" one. Then, λ_1 is determined by

$$\ln \delta(t)\sim\lambda_1 t; \quad \delta(t)\ll 1.$$

The values of λ_1 obtained in four different disturbance situations (Fig. 8) are given in Table I. One can see that all the values are close to each other and positive.

Similarly,

$$\ln V_2(t)\sim\lambda t.$$

Here, $\lambda=\lambda_1+\lambda_2$, and V_2 is a volume in a state space that can be defined in different ways. In order to calculate the volume V_2, we use various combinations of the pairs of the zooplankton vectors $\mathbf{h}^{(1)}(t)$, $\mathbf{h}^{(2)}(t)$, $\mathbf{h}^{(3)}(t)$, $\mathbf{h}^{(4)}(t)$, and $\mathbf{h}^{(0)}(t)$ specified as above. Here,

$$V_2=\sqrt{\det(CC^T)}$$

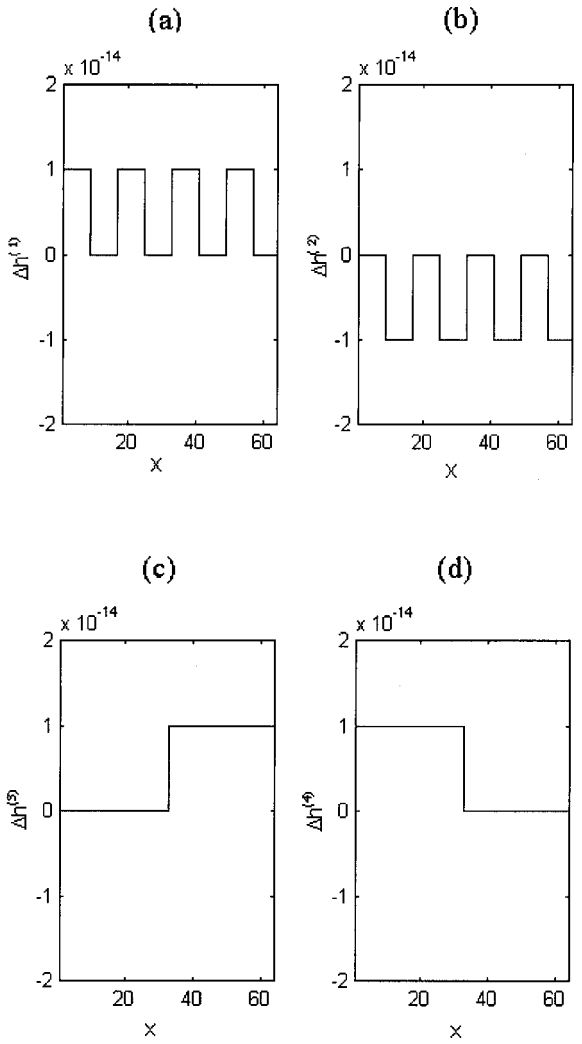

FIG. 8. Four types (a, b, c, and d) of the disturbances of the zooplankton distribution at the moment t_1 leading to the four different vectors $\mathbf{h}^{(1)}$, $\mathbf{h}^{(2)}$, $\mathbf{h}^{(3)}$, and $\mathbf{h}^{(4)}$ correspondingly.

where

$$C=\begin{pmatrix}\mathbf{v}\\ \mathbf{w}\end{pmatrix}=\begin{pmatrix}v_1 & \cdots & v_{64}\\ w_1 & \cdots & w_{64}\end{pmatrix},$$

the time-dependent vectors $\mathbf{v}$ and $\mathbf{w}$ are, for example, specified in the following way:

$$\mathbf{v}(t)=\mathbf{h}^{(0)}(t)-\mathbf{h}^{(1)}(t),$$

$$\mathbf{w}(t)=\mathbf{h}^{(0)}(t)-\mathbf{h}^{(2)}(t),$$

and C^T is the transposed matrix C. The second Lyapunov exponent

$$\lambda_2=\lambda-\lambda_1.$$

Examples obtained in such a way values of λ_2 (for $\lambda_1=0.0172$) are given in Table II. All these values are positive and obviously close to each other. The values of Lyapunov exponents λ_3 and λ_4 from the Lyapunov spectrum character-

izing the plankton dynamics are calculated in the similar way. All the values of λ_3 and λ_4 are also found to be positive.

The corresponding Lyapunov exponents for phytoplankton are also positive, which is not surprising since the phytoplankton dynamics is closely related to the zooplankton dynamics. Many authors have reported on an inverse relationship between phytoplankton and zooplankton densities, i.e., phytoplankton density is lower in the regions where zooplankton density is higher and *vice versa*. Such an inverse relationship is an apparent consequence of phytoplankton grazing by zooplankton (cf. [12]).

[1] V. Rai and W. M. Schaffer, Chaos, Solitons Fractals **12**, 197 (2001).
[2] J. A. Barth, J. Geophys. Res., [Oceans] **94(C8)**, 10 844 (1989).
[3] K. N. Fedorov, *The Structure of Ocean Fronts* (Gidrometeoizdat, Leningrad, 1983).
[4] M. J. Bowman, S. M. Chiswell, P. L. Lapennas, and R. A Murtagh, in *Coastal Oceanography*, Vol. 11 of *NATO Advanced Studies Institute Series IV: Marine Sciences*, edited by H. G. Gade *et al.* (Plenum Press, New York, 1983).
[5] L. Armi, D. Hebrt, N. Oakey, J. Price, P. L. Richardson, T. Rossby, and B. Ruddick, Nature (London) **333**, 649 (1988).
[6] E. Ranta, V. Kaitala, and P. Lundberg, Science **278**, 1621 (1997).
[7] A. B. Medvinsky, D. A. Tikhonov, J. Enderlein, and H. Malchow, Nonlinear Dyn., Psychol., Life Sci. **4**, 135 (2000).
[8] R. M. Nisbet, C. J. Briggs, W. Corney, W. W. Murdoch, and A. Stewart-Oaten, Lect. Notes Biomath. **96**, 125 (1993).
[9] A. M. Turing, Philos. Trans. R. Soc. London, Ser. B **237**, 37 (1952).
[10] L. A. Segel and J. L. Jackson, J. Theor. Biol. **37**, 545 (1972).
[11] S. A. Levin and L. A. Segel, Nature (London) **259**, 659 (1976).
[12] M. J. R. Fasham, Oceanogr. Mar. Biol. Ann. Rev. **16**, 43 (1978).
[13] P. J. S. Franks, J. S. Wroblewski, and G. R. Flieri, Mar. Biol. (Berlin) **91**, 121 (1986).
[14] O. A. Misund, H. Vilhjálmsson, S. Hjalti i Jákupsstovu, I. Røttingen, S. Belikov, O. Asthorsson, J. Jonsson, A. Krysov, S. A. Malmberg, and S. Sveinbjørnsson, SARSIA **83**, 117 (1998).
[15] J. H. Steel and E. W. Henderson, J. Plankton Res. **14**, 1397 (1992).
[16] A. Fernö, T. J. Pitcher, W. Melle, L. Nøttestad, S. Mackinson, C. Hollingworth, and O. A. Misund, SARSIA **83**, 149 (1998).
[17] J. E. Truscott and J. Brindley, Philos. Trans. R. Soc. London, Ser. B **347**, 703 (1994).
[18] D. W. Sims and V. A. Quayle, Nature (London) **393**, 460 (1998).
[19] E. R. Abraham, Nature (London) **391**, 577 (1998).
[20] H. Malchow and N. Shigesada, Nonlinear Processes in Geophysics **1**, 3 (1994).
[21] V. N. Biktashev, A. V. Holden, M. A. Tsyganov, J. Brindley, and N. A. Hill, Phys. Rev. Lett. **81**, 2815 (1998).
[22] H. Malchow, B. Radtke, M. Kallache, A. B. Medvinsky, D. A. Tikhonov, and S. V. Petrovskii, Nonlinear Analysis: Real World Application **1**, 53 (2000).
[23] I. A. Tikhonova, O. Arino, G. R. Ivanitsky, H. Malchow, and A. B. Medvinsky, Biophysics (Engl. Transl.) **45**, 343 (2000).
[24] M. Pascual and H. Caswell, J. Theor. Biol. **185**, 1 (1997).
[25] S. V. Petrovskii and H. Malchow, Math. Comput. Modell. **29**, 49 (1999).
[26] H. Malchow, Proc. R. Soc. London, Ser. B **251**, 103 (1993).
[27] H. Malchow, Ecol. Model. **75-76**, 123 (1994).
[28] M. Scheffer, Oikos **62**, 271 (1991).
[29] M. Pascual, Proc. R. Soc. London, Ser. B **251**, 1 (1993).
[30] A. Okubo, *Diffusion and Ecological Problems: Mathematical Models* (Springer, New York, 1980).
[31] M. Scheffer, J. Plankton Res. **13**, 1291 (1991).
[32] J. G. Skellam, Biometrika **38**, 196 (1951).
[33] S. E. Jørgensen, *Fundamentals of Ecological Modelling* (Elsevier, Amsterdam, 1994).
[34] M. Scheffer, Hydrobiol. Bull. **23**, 73 (1989).
[35] E. Steffen, H. Malchow, and A. B. Medvinsky, Environmental Modeling and Assessment **2**, 43 (1997).
[36] G. Sugihara and R. M. May, Nature (London) **344**, 734 (1990).
[37] D. A. Tikhonov, J. Enderlein, H. Malchow, and A. B. Medvinsky, Chaos, Solitons Fractals **12**, 277 (2001).